Investigating the experimental space for two-step Cu(In,Ga)(S,Se)$_2$ absorber layer fabrication: A design of experiment approach

Sarallah Hamtaei[1,2,3] , *Guy* Brammertz[1,2,3], *Thierry* Kohl[1,2,3], *Dilara* Gokcen Buldu[1,2,3], *Gizem* Birant[1,2,3], *Jessica* de Wild[1,2,3], *Marc* Meuris[1,2,3], *Jef* Poortmans[1,3,4,5] , *Bart* Vermang[1,2,3]

[1] Institute for Material Research (IMO), Hasselt University (partner in Solliance), Wetenschapspark 1, Diepenbeek, 3590, Belgium.
[2] imec division IMOMEC (partner in Solliance), Wetenschapspark 1, 3590 Diepenbeek, Belgium.
[3] EnergyVille, Thorpark 8320, Genk, 3600, Belgium.
[4] imec (partner in Solliance & EnergyVille), Kapeldreef 75, Leuven, 3001, Belgium.
[5] Department of Electrical Engineering, KU Leuven, Kasteelpark Arenberg 10, 3001 Heverlee, Belgium.

Abstract

This research reveals the missing or often undisclosed experimental data on processing conditions of Cu(In,Ga)(S,Se)$_2$ absorbers by the two-step sequential technique. Accordingly, by employing a one-variable-at-a-time approach- where each factor is exclusively changed with respect to a defined center point, we identified a handful of significant parameters which play the most significant role in an absorber's properties and consequently, prospective high-performing solar cells. This was done by analyzing their impact on a few most important metrics. Hence, the vast processing window with numerous factors and levels for development of Cu(In,Ga)(S,Se)$_2$ by this method becomes constrained and feasible to optimize in future endeavours.

Keywords

Copper indium gallium selenide sulfide, Two-step sequential processing, Design of Experiment

1. Introduction

There has been plenty of research on improving performance of solar cells based on Cu(In,Ga)(S,Se)$_2$ absorbers, hereafter referred to as CIGSSe, via i.a., surface treatment and alloying the absorber[1–3] and implementing alternative and additional layers surrounding the absorber[4]. Another approach has been focusing on improving absorbers by optimizing the

actual processing step of the absorber development. While most of such research focuses on absorbers fabricated by co-evaporation and multistep techniques, the two-step sequential processing, widely implemented by Avancis[5] and remarkably commercialized by Solar Frontier[5], still merits more attention. In this method of making these types of chalcogenide absorber layers, essentially a metal precursor of copper-gallium and indium is selenized (and/or sulfurized) with a solid or gaseous source. Next to valuable insights from the work of Intermolecular[6], some clarity on processing of pure selenide and pure sulfide variations of these chalcogenides has been recently offered by Solliane and imec, respectively[7,8]. On the other hand, as Kato et al. suggested[9], every tool and fabrication design might need its own process optimization for best results.

To such end, this is a preliminary study in a systematic approach to understand and optimize the two-step processing of CIGSSe-based solar cells. The idea here is to investigate the experimental space of the absorber development and identify the main impactful active factors therein.

2. Experimental details

Here, a 2.5*5 cm^2 Indium/ Copper Gallium/ Molybdenum/ Soda-lime glass (SLG) precursor is selenized and then sulfurized using hydrogen selenide (H_2Se) and hydrogen sulfide (H_2S) gases, respectively, to develop poly-crystalline CIGSSe absorber layers. SLG use as a rigid substrate is well established within the community as an affordable and practical choice which also provides (beneficial) light alkalis to the system[10]. The precursor had a bi-layer configuration of indium and cupper gallium layers, with a total of ~1 μm thickness, including the Molybdenum layer (Figure 1.a).

The samples were then annealed in a cold-wall chamber Annealsys AS-ONE rapid thermal processing system according to the following plan. An annealing profile was created (Figure 1,

left), wherein the system is first stabilized at 150°C for 1 minute . Samples are then pre-annealed in a N_2 atmosphere at a specific temperature, pressure, and duration. Here the aim is to remove native surface oxides and homogenize the precursor composition throughout the sample. Right after, H_2Se gas is introduced to the system just before and during ramping up the temperature to the second anneal (selenization anneal). The system's temperature is then ramped up to the final anneal value, where samples are introduced to H_2S at a high temperature (sulfurization anneal). In the end, the profile includes a controlled cooling phase in the H_2Se atmosphere before process termination. Consequently, CIGSSe films with ~1.5 μm thin films are made (Figure 1.b).

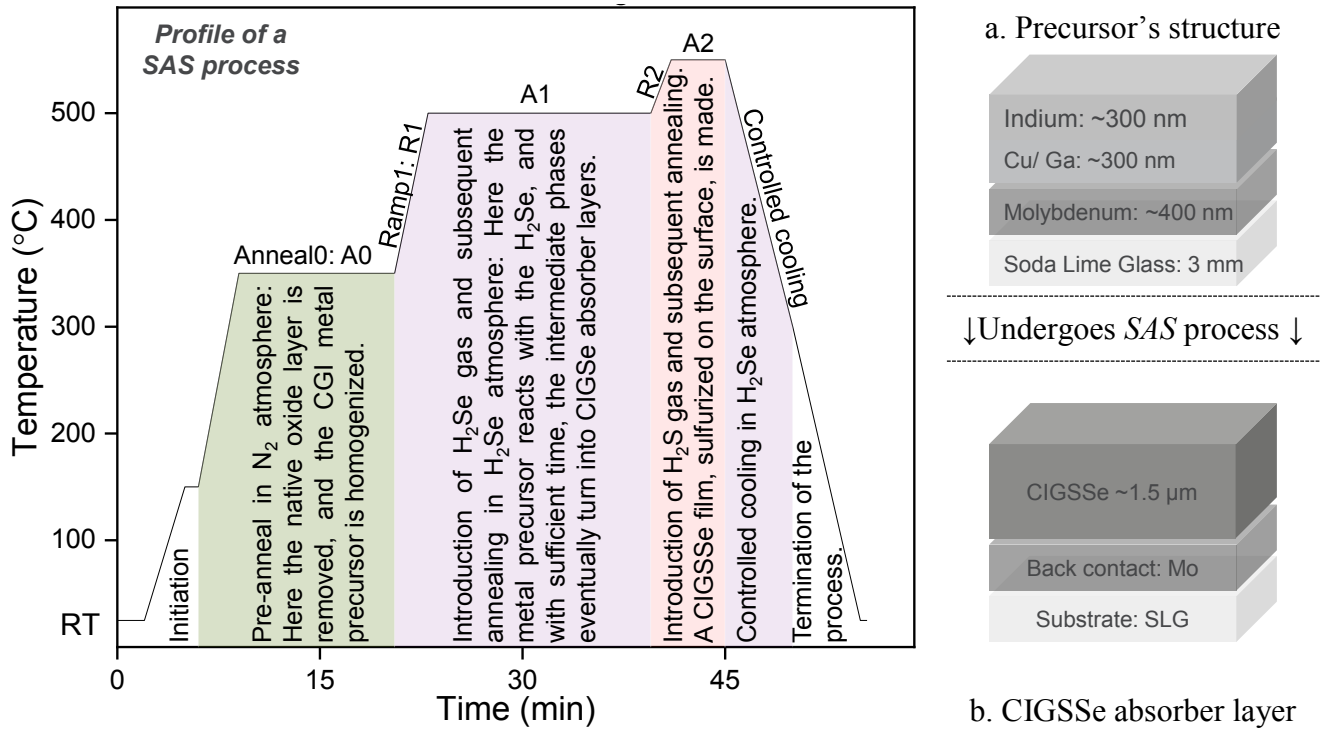

Figure 1.Precursor's structure (a) before undergoing the sulfurization after selenization anneal (SAS) (left) for processing precursors to CIGSSe absorber layers (b).

A vast number of processing factors may play a role in this profile. Such makes the application of factorial designs to screen their effects impractical. Thus, we made a list of possibly important parameters (Table 1) and employed a one variable at a time approach to screen their effect: Factors were first assigned a particular value based on the know-how of the group (Center Point

or simply CP), resulting in *an* active absorber layer- a baseline. Then, a lower and higher extreme level was assigned to each factor, respective to the CP, and an experiment was run per combination of levels, e.g., one run with all factors at the CP level, but Nitrogen Anneal (A0) at a higher temperature than CP. Note that no interactions are considered, and all experiments are designed only to understand the effect of individual factors. Furthermore, to understand the repeatability and reliability of our processing systems, the CP was repeated five times.

For ease of referral within the text and figures, these factors and their corresponding levels are *coded* as in Table 1. Lower and higher levels were chosen based on the extremes, limited by hardware and material constraints, e.g., higher annealing temperatures would damage the thermocouples used in the system. With such limits in mind, the levels were chosen to represent meaningful and possible extremes of each particular factor.

Table 1. Pre-anneal, selenization and sulfurization processing parameters and corresponding factor codes. Temp, amt, int, cool, and CP stand for Temperature, Amount, Introduction, Cooling, and Center Point, respectively.

Processing Phase	***Processing factor***	***Code***	***Level****		
			Low (-)	***CP***	***High (+)***
N_2 preanneal	A0 temp (°C)	A	290	350	400
	A0 dur (sec)	B	0	15	30
Introducing H_2Se	H_2Se amt (KPa)	C	>2	>4	>50
	H_2Se int flow (sccm)	D	100	300	900
Ramp to Selenization	R1 Rate (°C/s)	E	0.2	1	5
Selenization anneal	H_2Se flow (sccm)	F	0	20	50
	A1 dur (min)	G	2	15	30
	A1 temp (°C)	H	450	500	530
Introducting H_2S	H_2S amt (KPa)	I	>2	>4	>20
	H_2S int flow (sccm)	J	100	300	900
Ramp to Sulfurization	R2 rate (°C/s)	K	0.4	2	10
Sulfurization anneal	A2 dur (min)	L	1	3	9
	A2 temp (°C)	M	505	550	600
Cooling	Cool rate (°C/s)	N	0.2	1	0.5
	Cool H_2Se flow (sccm)	O	0	20	100

*Low and high extreme levels of each factor were tested with all other variables maintained at the CP level.

With minimum time after the processing, the samples were characterized in different metrics. Microstructural and composition analysis was carried out under scanning electron microscopy

(SEM) and energy-dispersive X-ray spectroscopy (EDX) with a Tescan and Bruker SEM system. Both of these were done at 15kV operating voltage. For EDX, measurements were done on specific features of interest which were in the scale of few micrometers. Surface roughness was measured under Keyence's laser scanning microscope. Additionally, Optical bandgap, photoluminescence (PL) intensity, and corresponding minority carriers' lifetime decay component (LT), were assessed as other quantitative metrics. Effective bandgap was chosen as an important metric, because it indicates suitability of the produced absorber for single and/ or multi junction solar cell devices. Furthermore, high lifeitme (and PL intensity) and low surface roughness are interesting aspects in assessing the quality of absorbers, in that they imply an absorber with less defects. These measurements were done under a Picoquant FluoTime 300 photoluminescence spectroscopy micro system with an excitation wavelength of 532 nm (25 ps, 3 MHz). This was done on bare CIGSSe absorbers, at room temperature, and after an average of 30 seconds exposure time between their fabrication and measurment.

Active factors were then identified by comparing these properties against that of the CP. Measurements were done on at least three points per sample to increase the validity of inferences.

3. Results and discussion

The discussion is provided for qualitative and quantitative metrics separately. However, common to our analysis in both is that identifying the dominant factors is done considering their *absolute* impact (e.g., not necessarily towards lowest surface roughness, or towards a microstructurally smooth surface). The section is concluded with a note on response curvature.

3.1. Qualitative metrics

Figure 2 contains representative instances of microstructural features visible under SEM throughout the experimental run. These features have appeared solely or in combination with each other and with various densities on the surface of samples within the experimental run. The precursor's bilayer configuration suggests that indium particles (Figure 2. Precursor) have served as a favorable nucleation site for forming CIGSSe films with small grains at the order of 1 µm (Figure 2.b). A *bump* is visible on the surface of some films (Figure 2.a- note the difference in height on either side of the image), which could be due to partial delamination of sublayers or agglomeration of indium particles on different locations[6].

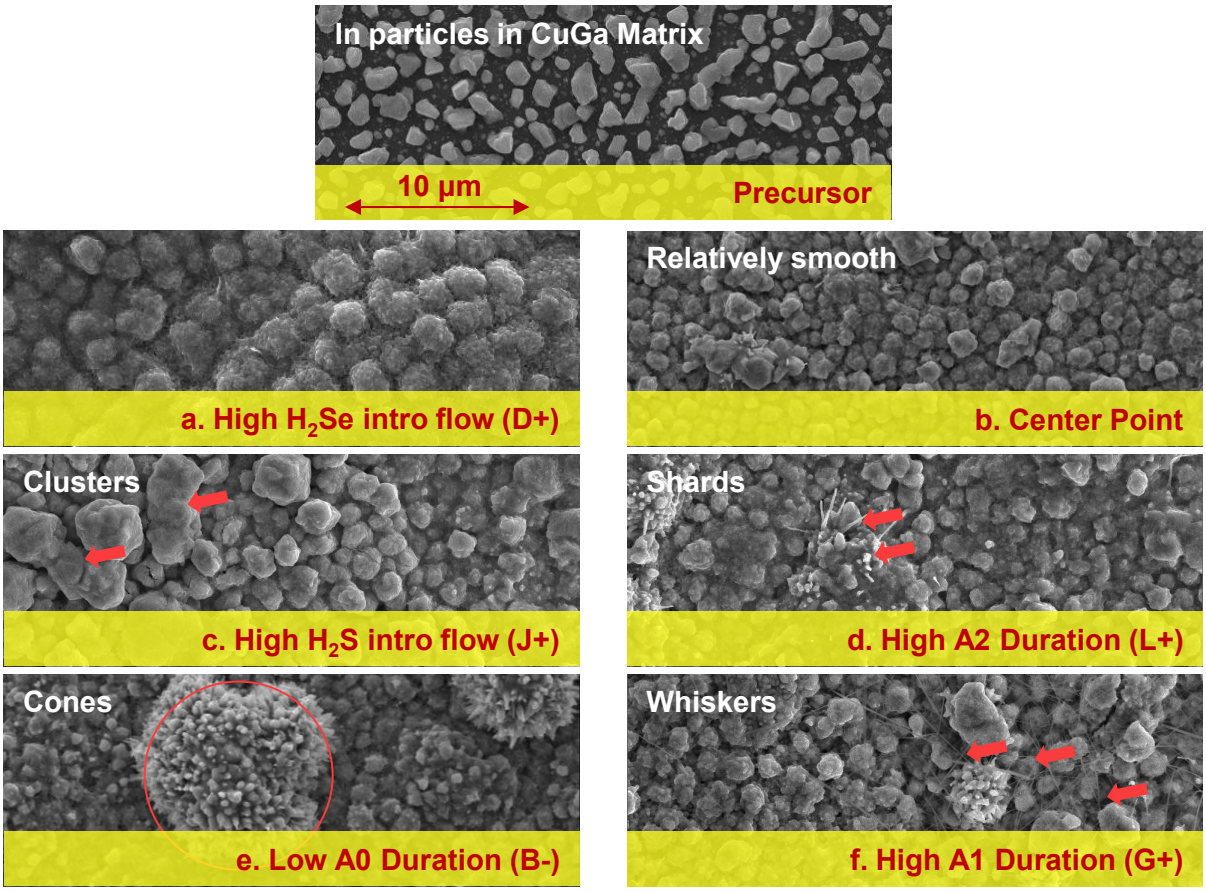

Figure 2. Representative instances of microstructural features appeared in the experimental run under top view SEM.

Another notable feature was the *clustering* of CIGSSe grains (Figure 2.c). Next to these, a feature that appeared occasionally was *shards* (Figure 2.d), upon which we assume cones evolve. These nanometer high features contain zero gallium and high amounts of Selenium and Sulfur under EDX measurement (Figure 2.e).

Lastly, *whiskers* occur in a few samples (Figure 2.f), which are too narrow and thin to analyze their composition under EDX. This was only primarily pronounced on two occasions: when there was a long A1 anneal and when sulfurization temperature was increased to the extreme of 600°C.

Table 2. Summary of most notable microstructural features for each sample and factor. Wh stands for whiskers. (See Table 1 for factor codes)

Factor code	microstructural feature						Factor code	microstructural feature						Total score
	Smooth	Cluster	Bump	Shard	Cone	Wh		Smooth	Cluster	Bump	Shard	Cone	Wh	
A-					xx		A+					xx		4
B-					xx		B+					x		3
C-				x	x		C+			x				3
D-					x		D+			x		x		3
E-			x				E+				x	x		3
F-			x				F+		x	x		x		4
G-	x						G+					xx	x	4
H-	xx						H+				x	xx		5
I-					x		I+				x	x		3
J-		x					J+	x	x					3
K-					x		K+					x		2
L-	x						L+		x		x			3
M-				x			M+		x	x		x	x	5
N-					x		N+	x		x				3
O-		x	x				O+	x						3

3.2. Quantitative metrics

Quantitative results for all the samples set in the experimental run consist of PL peak position and intensity, lifetime decay component, and surface roughness. These are plotted for all the data in Figure 3 and serve as a visual aid to see their overall distribution.

With an expected value of 1204 nm (~1.03 eV) and a coefficient of variation- CV, defined as the ratio of standard deviation to average value, of 0.013, the PL peak position proved to be relatively robust to changing processing parameters within their designed range. This would

suggest formation of a Ga back graded low bandgap CIS film which is in line with obtained bandgap values from PL data.This is not surprising given that Gallium (an agent to increase bandgap in CIGSSe absorbers) is known to segregate towards the back surface in the two-step processing method[11].

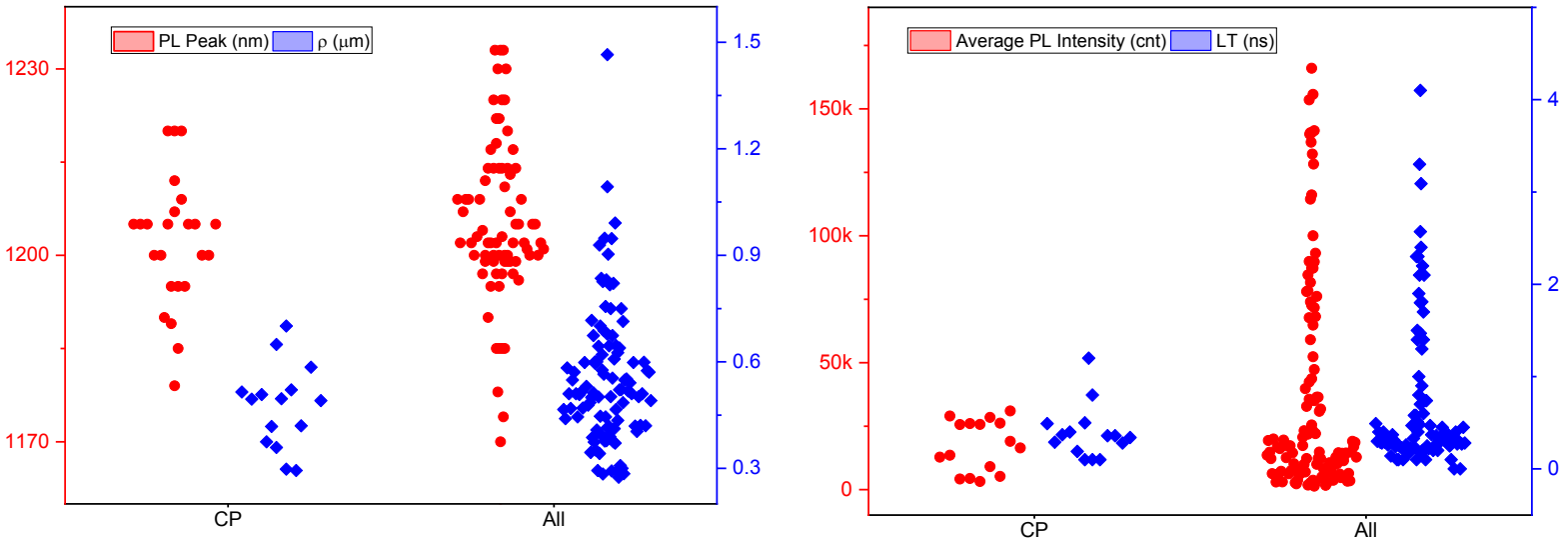

Figure 3. General distribution of the results for all the experimental run compared to the Center Point.

Thus, these materials can be potentially employed as an ideal bottom cell in tandem photovoltaics. Given the very small variation in PL peak data (low CV), it was concluded that the processing chosne processing parameters and/or their respective levels could not individually affect the bandgap of our absorbers. Therefore, we excluded the peak position metric for the rest of the analysis to find most impactful factors.

Table 3.Statistics of data dispersion. Extreme outliers are cleaned from the data.

Statistic	Metric			
	PL peak (nm)	PL intensity (counts)	Lifetime (ns)	Roughness (μm)
CP's average	1202	17500	0.29	0.45
CP's CV	0	0.5	0.4	0.2
Total Average	1204	37000	0.72	0.53
Total CV	0.013	1.162	1.15	0.29

However, changing the factors has caused a significant change to the CP results in LT and PL intensity, and to a less extent, in roughness (See Table 3). The latter could be attributed to the

high roughness characteristic of two-step processed CIGSSe absorbers[12]. Consequently, roughness response is treated with less weight in further analysis and only when other metrics did not respond well.

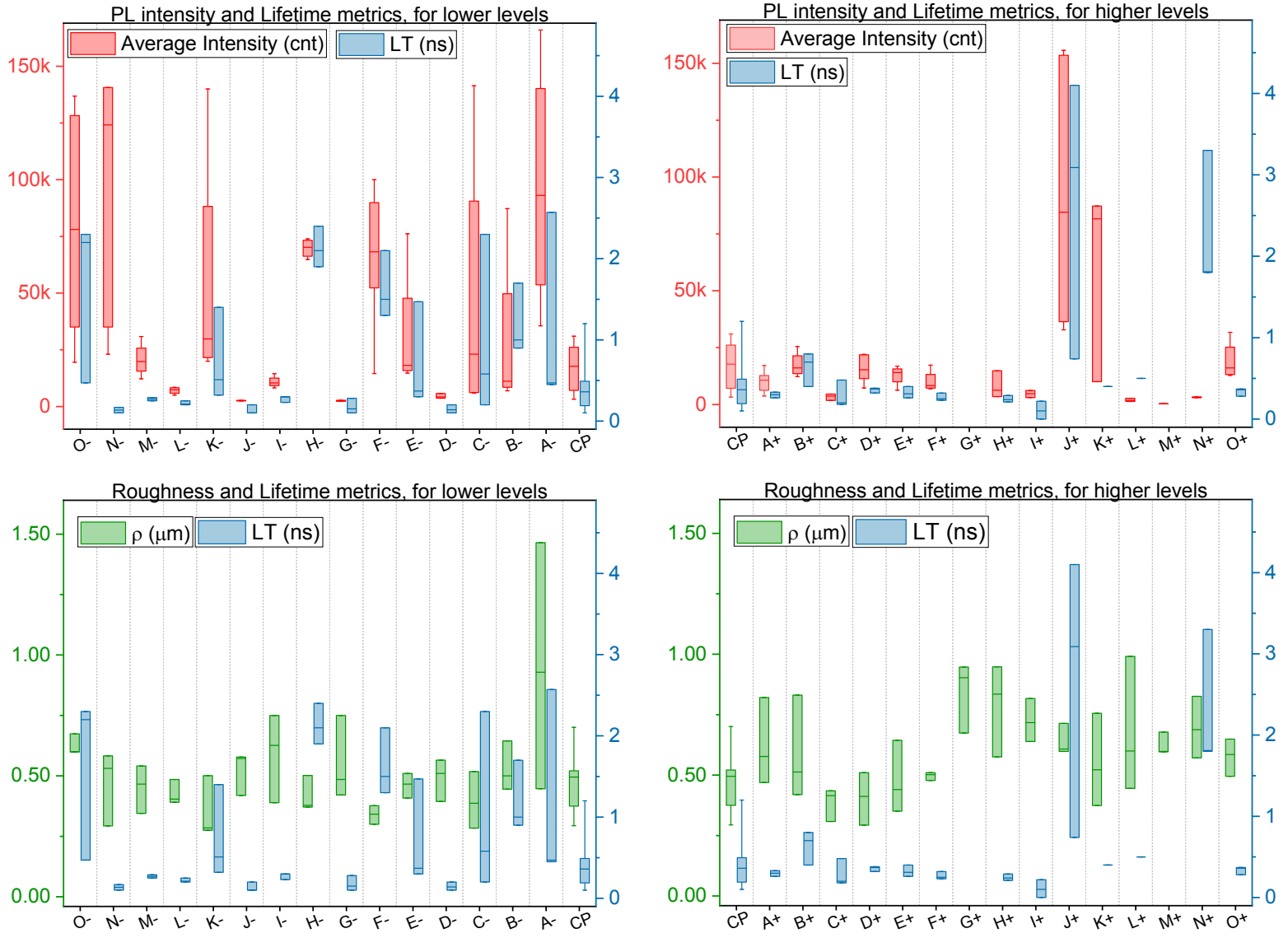

Figure 4. PL intensity and lifetime metrics, for each factor at lower and higher levels, with respect to CP.

To this end, more detailed results for LT and intensity for each factor at low and high levels were illustrated in a box plot (Figure 4). To save space, code names are used instead of the factor name- See Table 1 for reference.

Looking at the data, one can cast factors lying outside the CP's range (represented by whiskers in the box plot) as impactful parameters. That is factors A, F, G, H, J, and O. Among these, G's impact, when it is on a higher level than CP, works towards decreasing LT to the extent of nullifying it. Such also occurs but to a less extent in the case of factor M at a higher level.
As this categorization is mainly based on LT and intensity, these two interconnected metrics must point in the same *direction* or lie inside or outside the CP's range. Thus, the impact of factors N and K were cast inconclusive due to discrepancies between the two mentioned metrics. Focusing on surface roughness, only changing factors A, G, H and L have resulted in a relatively significant change to the CP's value. Such could be attributed to the density and variety of microstructural features on their surface- See Table 2.

3.3. Curvature in response

By having a low, CP and high level for each of the processing parameters, it was possible to roughly estimate the presence of interactive factor, i.e., the presence of curvature in response, by fitting a linear regression model and evaluating the R squared and adjusted R squared statistics (the latter corrects the former by the number of independent variables).

Table 4.Linearity statistics for a simple regression model of LT and PL intensity response variables

Metric	Statistic (%)	Factor codes- see Table 1for reference.								
		A	F	G	H	J	K	M	N	O
LT	R^2	51	72	23	90	97	37	48	~0	77
	R^2_{adj}	3	44	-	81	95	-	-	-	54
PL intensity	R^2	74	74	~0	93	99	20	91	73	39
	R^2_{adj}	48	48	-	87	98	-	82	47	-

These are reported in Table 4 for factors shortlisted above and only for LT and PL intensity. According to the linear regression model, only factors H and notably J show strong indications of linearity. Therefore, it can be concluded that they are not interacting with other processing

parameters. The rest of the factors either showed low or even negative values of statistic, implying presence of curvature in response curves.

4. Conclusion

Six significant factors in the two-step processing of CIGSSe absorber layers, by use of gaseous H_2Se and H_2S, were identifie. These are explained as follows, in order of appearance in the thermal processing of metal precursors. Temperature of a Nitrogen pre-anneal on the precursor; The flow rate at which the H_2Se is introduced in the heat-up ramp to selenization anneal; The selenization anneal's duration; The selenization anneal's temperature; The introduction flow of H_2S at the end of selenization anneal- latter two factors indicated linearity in their response (within the respective investigated range of levels), which implies their lack of interaction with other parameters. The last important processing factor was the H_2Se flow in the cooling stage of the anneal. We were not able to reliably conclude on two other factors: the heat-up ramp rate to the sulfurization anneal and the cooling rate at the end of the process. Therefore, these two should still be considered in future studies. These results already narrow down the experimental space wherein one can design and optimize the fabrication route of $Cu(In,Ga)(S,Se)_2$ thin film absorbers.

Acknowledgments

This study has received funding from the European Union's Horizon 2020 research and innovation program under grant agreement No. 850937 (PERCISTAND), and by the Social Research Fund (BOF) from Hasselt University, under BOF20OWB07.

References

[1] S. Siebentritt, E. Avancini, M. Bär, J. Bombsch, E. Bourgeois, S. Buecheler, R. Carron, C. Castro, S. Duguay, R. Félix, E. Handick, D. Hariskos, V. Havu, P. Jackson, H.-P. Komsa, T. Kunze, M. Malitckaya, R. Menozzi, M. Nesladek, N. Nicoara, M. Puska, M. Raghuwanshi, P. Pareige, S. Sadewasser, G. Sozzi, A.N. Tiwari, S. Ueda, A. Vilalta- Clemente, T.P. Weiss, F. Werner, R.G. Wilks, W. Witte, M.H. Wolter, Heavy Alkali Treatment of Cu(In,Ga)Se2 Solar Cells: Surface versus Bulk Effects, Advanced Energy Materials. 10 (2020) 1903752. https://doi.org/10.1002/aenm.201903752.

[2] Y. Zhang, Z. Hu, S. Lin, C. Wang, S. Cheng, Z. He, Z. Zhou, Y. Sun, W. Liu, Silver Surface Treatment of Cu(In,Ga)Se $_2$ (CIGS) Thin Film: A New Passivation Process for the CdS/CIGS Heterojunction Interface, Sol. RRL. 4 (2020) 2000290. https://doi.org/10.1002/solr.202000290.

[3] D.G. Buldu, J. de Wild, T. Kohl, G. Brammertz, G. Birant, M. Meuris, J. Poortmans, B. Vermang, Study of Ammonium Sulfide Surface Treatment for Ultrathin Cu(In,Ga)Se $_2$ with Different Cu/(Ga + In) Ratios, Phys. Status Solidi A. 217 (2020) 2000307. https://doi.org/10.1002/pssa.202000307.

[4] G. Birant, J. de Wild, T. Kohl, D.G. Buldu, G. Brammertz, M. Meuris, J. Poortmans, B. Vermang, Innovative and industrially viable approach to fabricate AlOx rear passivated ultra-thin Cu (In, Ga) Se2 (CIGS) solar cells, Solar Energy. 207 (2020) 1002–1008.

[5] F. Karg, High Efficiency CIGS Solar Modules, Energy Procedia. 15 (2012) 275–282. https://doi.org/10.1016/j.egypro.2012.02.032.

[6] H. Liang, U. Avachat, W. Liu, J. van Duren, M. Le, CIGS formation by high temperature selenization of metal precursors in H2Se atmosphere, Solid-State Electronics. 76 (2012) 95–100. https://doi.org/10.1016/j.sse.2012.05.055.

[7] M. van der Vleuten, M. Theelen, R. Aninat, K. van der Werf, H. Mannetje, P. Reyes-Figueroa, T. Kodalle, R. Klenk, M. Simor, H. Linden, Control over the Gallium Depth Profile in 30×30 cm2 Sequentially Processed CIGS, in: 2020 47th IEEE Photovoltaic Specialists Conference (PVSC), 2020: pp. 0640–0645. https://doi.org/10.1109/PVSC45281.2020.9300963.

[8] S. Hamtaei, G. Brammertz, M. Meuris, J. Poortmans, B. Vermang, Dominant Processing Factors in Two-Step Fabrication of Pure Sulfide CIGS Absorbers, Energies. 14 (2021) 4737. https://doi.org/10.3390/en14164737.

[9] T. Kato, Cu(In,Ga)(Se,S)2 solar cell research in Solar Frontier: Progress and current status, Jpn. J. Appl. Phys. 56 (2017) 04CA02. https://doi.org/10.7567/JJAP.56.04CA02.

[10] V. Petrova-Koch, R. Hezel, A. Goetzberger, High-efficient low-cost photovoltaics, Springer, 2008. https://doi.org/10.1007/978-3-540-79359-5.

[11] G.M. Hanket, W.N. Shafarman, B.E. McCandless, R.W. Birkmire, Incongruent reaction of Cu–(InGa) intermetallic precursors in H 2 Se and H 2 S, Journal of Applied Physics. 102 (2007) 074922. https://doi.org/10.1063/1.2787151.

[12] Y. Kamikawa, J. Nishinaga, H. Shibata, S. Ishizuka, Efficient Narrow Band Gap Cu (In, Ga) Se2 Solar Cells with Flat Surface, ACS Applied Materials & Interfaces. 12 (2020) 45485–45492. https://doi.org/10.1021/acsami.0c11203.

List of figures and tables